Title
Gap in the magnetic excitation spectrum of Ce3Bi4Pt3

Journal
Physical Review B, 44(13)

ISSN
2469-9950

Authors
Severing, A
Thompson, JD
Canfield, PC
et al.

Publication Date
1991-10-01

DOI
10.1103/physrevb.44.6832

Gap in the magnetic excitation spectrum of $Ce_3Bi_4Pt_3$

A. Severing
Institut Laue-Langevin, Grenoble, France

J. D. Thompson, P. C. Canfield, and Z. Fisk
Los Alamos National Laboratory, Los Alamos, New Mexico 87545

P. Riseborough
Polytechnic University, Brooklyn, New York 11201
(Received 9 May 1991)

Static-susceptibility and thermal-expansion measurements indicate that $Ce_3Bi_4Pt_3$ is mixed-valent-like, whereas transport measurements reveal a gap of $\Delta = 5$ meV in the electronic excitation spectrum. We report the magnetic response of $Ce_3Bi_4Pt_3$, at temperatures between 2 and 150 K, determined with incident neutron energies of 3.1, 17, and 69 meV. The isostructural, nonmagnetic reference compound $La_3Bi_4Pt_3$ was also studied at the same temperatures and energies so that phonon contributions could be subtracted accurately. At 2 K, a gap $\Delta_m = 12$ meV is present in the magnetic excitation spectrum: the 3.1-, 17-, and 69-meV data consistently show that the magnetic intensity is zero for energy transfers less than 12 meV, rises sharply between 12 and 20 meV, and falls off smoothly beyond. Above 50 K, the gap in the spin-spin correlation function starts to fill. The neutron results reproduce the temperature dependence of the bulk susceptibility. The relationship between these and other measurements will be discussed.

INTRODUCTION

Most of the heavy-fermion or intermediate-valence compounds have a metallic ground state which is either paramagnetic, antiferromagnetic, or superconducting, and only a few $4f$ compounds show insulating behavior at low temperature with a small energy gap Δ in the electronic excitation spectra. $Ce_3Bi_4Pt_3$ appears to be intermediate valence and belongs to the insulating group.[1] The static susceptibility χ_{stat} is typical for an intermediate-valence compound, i.e., at high temperatures it has Curie-Weiss behavior, goes through a broad maximum at $T = 80$ K, and reaches a finite value for $T \rightarrow 0$ (see Fig. 1). The Curie tail at low temperatures may be attributed to sample impurities and/or defects. Thermal expansion measurements support the classification of $Ce_3Bi_4Pt_3$ as a possibly intermediate-valence compound.[2] The linear coefficient γ of the specific heat for $Ce_3Bi_4Pt_3$ is only 3.3 mJ/mol Ce K^2, which is three times smaller than that of $La_3Bi_4Pt_3$, and considerably smaller than the γ value expected from Bethe-ansatz analysis of the static susceptibility ($\gamma_{Bethe} = 75$ mJ/mol Ce K^2).[1] The semiconducting ground state of $Ce_3Bi_4Pt_3$ explains the absence of a significant electronic contribution to the specific heat. Below 50 K the resistivity rises sharply, and is clearly nonmetallic.[1] Altogether, transport properties can be described with an activation energy Δ of the order of 5 meV. Other $4f$ compounds with insulating ground states are TmSe ($\Delta \approx 2$ meV),[3] SmB_6 ($\Delta \approx 3$–4 meV),[4] YbB_{12} ($\Delta \approx 6$ meV),[5] $CeFe_4P_{12}$ ($\Delta \approx 130$ meV),[6] CeNiSn ($\Delta \approx 0.5$ meV),[7] and CeRhSb ($\Delta \approx 0.4$ meV).[8] Some of these compounds have intermediate valence.

The magnetic excitation spectra of $4f$ compounds with a metallic ground state have been intensively studied and the different behaviors can be summarized as follows: in the absence of any hybridization between $4f$ and conduction electrons, the magnetic excitation spectrum consists of a series of sharp quasielastic and inelastic lines, corresponding to the transitions between energy levels of the crystal-field split Hund's rule ground state. The temperature dependence of the linewidths follows a Korringa law (e.g., strongly diluted systems).[9–11] When hybridization sets in, the crystal-field splitting survives at first, but the

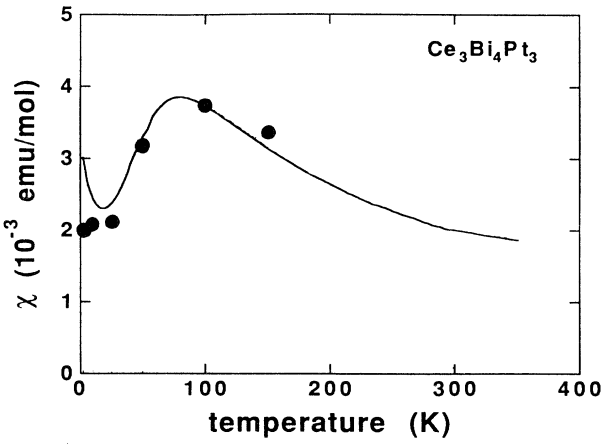

FIG. 1. Bulk susceptibility of $Ce_3Bi_4Pt_3$ vs temperature as measured in a SQUID magnetometer (line). The solid circles are the susceptibility values calculated from the neutron data, scaled to the magnetometer value at $T = 100$ K.

quasielastic and inelastic lines broaden as a result of the hybridization. The linewidths are finite for $T \rightarrow 0$ and increase strongly with temperature. Often the temperature dependence of the quasielastic line width is described by a square-root law ($\Gamma/2 \approx a + bT^{1/2}$), and its extrapolated zero-temperature value defines the so-called Kondo temperature [e.g., $CeAl_2$ and $CeCu_2Si_2$,[12] or $YbAuCu_4$ (Ref. 13)]. The spectra of these compounds can still be described with a crystal-field theory based on the assumption that the charge distributions which cause the crystal-field potential and the $4f$ wave functions do not overlap. In the extreme case of hybridization, i.e., in the intermediate-valence region, the crystal-field splitting of the Hund's-rule ground state, in the classical sense, breaks down. The neutron-scattering spectra are very broad and without much structure. At low temperatures, the magnetic intensity peaks at energy transfers which are significantly larger than expected from the largest energy splitting of an extrapolated crystal-field scheme. The spectral widths vary little with temperature. Examples are $CePd_3$,[14] $Ce(Pd_{1-x}Ag_x)_3$,[15] $\alpha-Ce_{0.8}Th_{0.2}$,[16] $YbInCu_4$,[17] and $YbAl_3$.[18] Often it is difficult to determine whether the magnetic intensity is zero at small energy transfers, i.e., whether the magnetic excitation spectra exhibit a gap Δ_m. The strongest indication for the existence of such a gap was found in metallic $YbAl_3$ ($\Delta_m \approx 30$ meV).[18,19]

Until recently there have been few neutron data available of $4f$ compounds with an insulating ground state. The existing data will be discussed together with the $Ce_3Bi_4Pt_3$ data in a later section.

EXPERIMENT AND ANALYSIS

$Ce_3Bi_4Pt_3$ and $La_3Bi_4Pt_3$ grow in small single crystals $1\times1\times5$ mm^3 out of a Bi flux. In this experiment we used about 30 g of powdered single crystals. The cubic ($I\bar{4}3d$) symmetry, with lattice constants of $a_0 = 10.051$ and 10.130 Å for the Ce and La sample,[2] was verified by x-ray diffraction. The static susceptibility was measured on a number of single crystals from our samples to assure that the magnetic properties are identical to the ones previously reported.[1]

The inelastic-neutron-scattering measurements were performed at the Institut Laue-Langevin in Grenoble on the time-of-flight spectrometers IN4 and IN6. These enabled us to investigate the inelastic and quasielastic part of the spectrum with different resolutions. Three different incident energies were used: $E_0 = 69$ and 17 meV on IN4, and $E_0 = 3.1$ meV on IN6. The respective energy resolutions are $\Delta E/E = 4.5\%$ on IN4 (FWHM) and 3% on IN6 at the elastic position. The IN4 resolution function does not vary with the energy transfer; the IN6 resolution can be considered as constant within an energy window of ± 2 meV. For the data correction we measured the empty sample holder, cadmium, and a vanadium standard in the sample position. All data shown are corrected for background, absorption, detector efficiency and are scaled to absolute units of cross section by the vanadium standard. The momentum transfer Q varies with the energy transfer, and the data points of the magnetic spectra are not corrected for the magnetic form factor $f(Q)$. However, fits to the magnetic spectra take the Ce^{3+} form factor into account for each time-of-flight channel and detector (i.e., before the detector grouping). In the spectra we always give the momentum transfer at the elastic position.

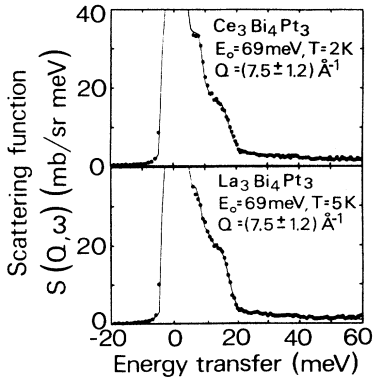

FIG. 2. $Ce_3Bi_4Pt_3$ and $La_3Bi_4Pt_3$ spectra at large scattering angles ($2\Theta = 82°$).

The nonmagnetic, isostructural compound $La_3Bi_4Pt_3$ was measured at the same temperatures and energies as the cerium sample in order to subtract the phonon scattering as accurately as possible. The lanthanum measurements show that only the 69-meV data contain a major phonon contribution. The high-Q data verify that the positions and widths of the phonon peaks are the same for the cerium and lanthanum samples (see Fig. 2). Therefore, we could fix the phonon positions and widths for the low-Q cerium data from fits to the lanthanum data. In order to determine the phonon intensities in the low-Q data of $Ce_3Bi_4Pt_3$, we tried two methods. (I) The intensities in the low-Q cerium data were determined with reference to the low-Q data of the lanthanum sample, allowing for the difference in the averaged nuclear scattering length [$\sigma_{av}(Ce) \approx 0.8\ \sigma_{av}(La)$]. (II) The lanthanum data yield a Q scaling for the phonon intensities, i.e., the ratio of the high-Q to low-Q phonon intensities. The multiplication of the high-Q cerium data with the inverse ratio should yield the low-Q phonon intensities, under the assumption that the high-Q data contain only phonon and no magnetic scattering. Method II leads to about 10% higher phonon intensities (total integrated intensity) for the low-Q Ce data relative to method I. The latter is due to the fact that the square of the Ce^{3+} magnetic form factor $|f(Q)|^2$ is not zero in the high-Q spectrum [$|f(Q) = 7.5\ \text{Å}^{-1}|^2 \approx 0.1$], i.e., assuming it to be wholly phononic leads to an overestimation of the phonon intensity. Therefore, we applied method I.

RESULTS

In Fig. 3, spectra of $Ce_3Bi_4Pt_3$ and $La_3Bi_4Pt_3$ are shown for small momentum transfers and several temperatures between 2 and 150 K. The lanthanum data contain only nuclear scattering, i.e., incoherent elastic and phonon scattering, whereas the cerium data contain magnetic

scattering in addition. The lanthanum spectra at low-Q [Figs. 3(g)–3(k)] and the high-Q data in Fig. 2 establish that most of the phonon scattering occurs at energy transfers smaller than 20 meV; the high-energy tail is probably due to multiple phonon scattering. Due to the Bose factor, the phonon intensities increase slightly with increasing temperature [Figs. 3(g)–3(k)]. In order to separate the magnetic from the nuclear scattering in the cerium data, the incoherent elastic peak has been described by the resolution function (vanadium) and the phonon intensities have been determined quantitatively according to method I described in the previous section. The result of the nuclear description is visualized by the solid lines in Figs. 3(a)–3(f). After subtracting the nuclear intensities, we are left with the purely magnetic spectra [see Figs. 4(a)–4(f)]. Since the elastic peak is about 25 times higher than the inelastic signal, this subtraction yields huge error bars in the elastic region (see open circles).

According to Fig. 4(a), the magnetic intensity at 2 K is zero for energy transfers smaller than 12 meV. Between 12 and 20 meV, the intensity rises sharply, and falls off smoothly beyond. Neither the spectrum's shape nor the width of the magnetic gap, $\Delta_m \approx 12$ meV, changes when warming up to 25 K [Figs. 4(b) and 4(c)]. At 50 K the magnetic gap is already partially filled, whereas the intensity at the high-energy edge of the spectrum starts to decrease [Fig. 4(d)]. Generally, the intensity shifts towards smaller energy transfers upon warming. At 100 and 150 K, the spectra appear almost like a broad quasielastic distribution [Figs. 4(e) and 4(f)].

Since the observation of a gap in the magnetic excitation spectrum for $T \leq 25$ K and the rapid change of the spectrum between 25 and 100 K is a rather unusual result, we wanted to underpin the data presented above. We performed measurements with smaller incident energies, i.e., with better resolution, in order to rule out the

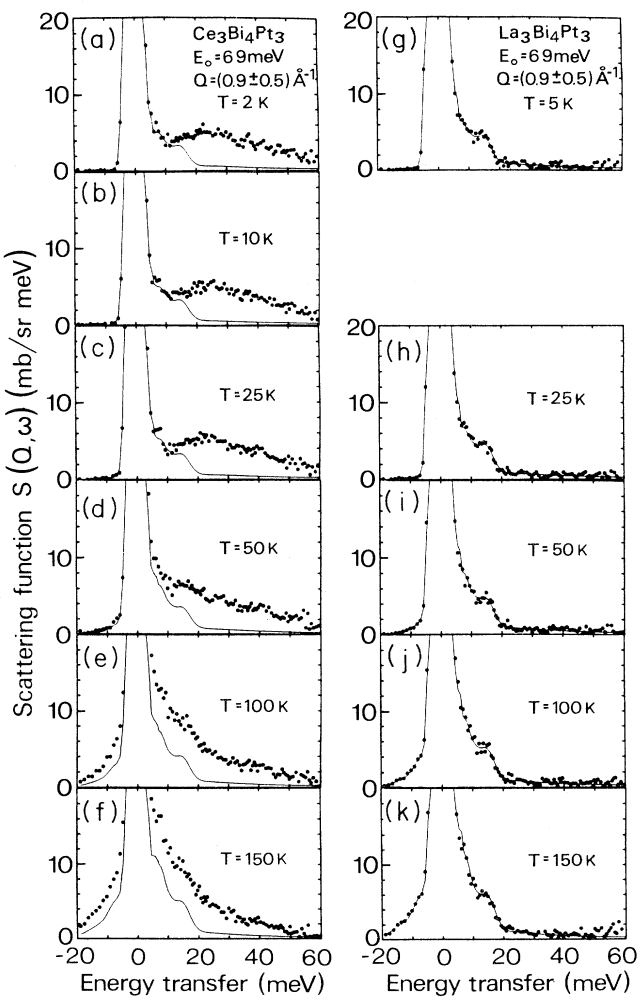

FIG. 3. (a)–(f) $Ce_3Bi_4Pt_3$ and (g)–(k) $La_3Bi_4Pt_3$ spectra for several temperatures at small scattering angles ($2\Theta = 8.4°$). The solid lines include the nuclear intensities, i.e., incoherent elastic and phonon scattering.

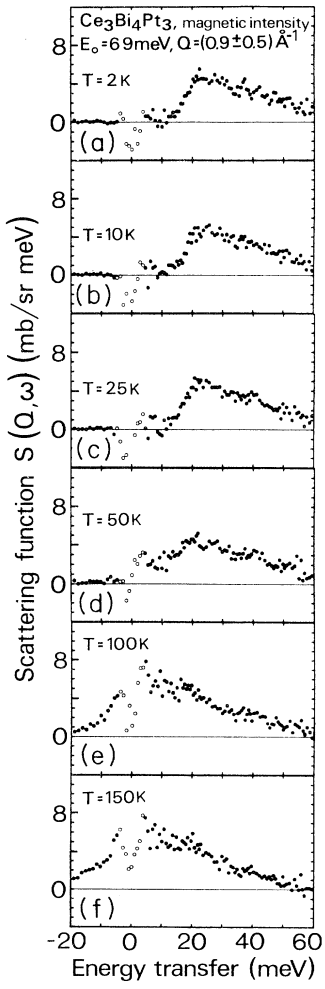

FIG. 4. $Ce_3Bi_4Pt_3$ spectra at small scattering angles ($2\Theta = 8.4°$) after subtraction of the nuclear scattering [areas under the lines in Figs. 3(a)–3(f)]. The open circles mark the elastic region in which the error bars are enormous due to the subtraction.

chance that we missed magnetic intensity within the resolution width. In Fig. 5, spectra of $Ce_3Bi_4Pt_3$ (solid circles) and $La_3Bi_4Pt_3$ (open squares) are shown, measured with an incident energy of 17 meV at the same temperatures as the 69-meV data. Here, we have not subtracted any nuclear scattering; the differences of the Ce and La spectra represent the magnetic intensity (the La data should be multiplied by the ratio of the nuclear scattering lengths to be more accurate). These data are consistent with the 69-meV data, i.e., below 25 K the magnetic intensity is zero within the displayed energy window (≤ 12 meV), and increases between 50 and 150 K. Additional measurements with even better resolution ($E_0=3.1$ meV) confirm that there is no magnetic intensity between 0.1 and 1.8 meV for temperatures below 25 K.

The ability of the data to yield the bulk susceptibility χ_{bulk} is a good verification of magnetic neutron results. The paramagnetic scattering function $S(Q,\omega)$ is related to the imaginary part of the dynamic susceptibility

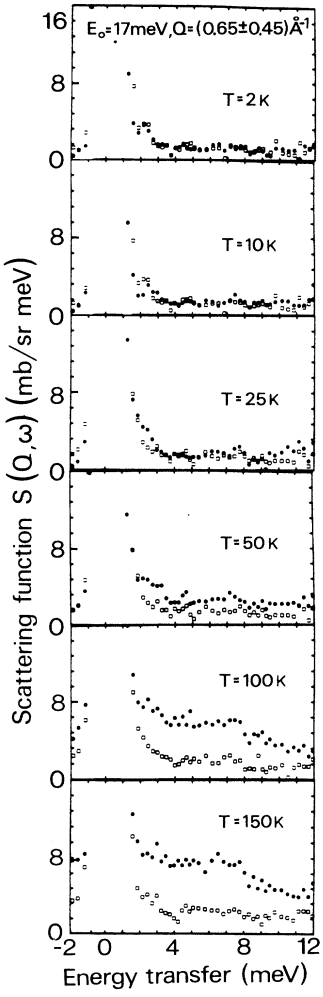

FIG. 5. 17-meV spectra of $Ce_3Bi_4Pt_3$ (●) and $La_3Bi_4Pt_3$ (□) for several temperatures at small scattering angles ($2\Theta=8.4°$). The difference in intensity between the Ce and La spectra is due to magnetic scattering.

$\chi''(\mathbf{Q},\omega)$, and the latter again can be expressed in terms of the bulk susceptibility via the Kramers Kronig relation:

$$S(Q,\omega)\approx(1-\exp[-\hbar\omega/kT])^{-1}\chi''(\mathbf{Q},\omega)$$
$$\approx\pi h\omega(1-\exp[-\hbar\omega/kT])^{-1}$$
$$\times|f(Q)|^2P(\mathbf{Q},\omega)\chi_{\text{bulk}}\,. \quad (1)$$

$P(\mathbf{Q},\omega)$ is a spectral function which has to fulfill the normalization requirement $\int_{-\infty}^{\infty}P(\mathbf{Q},\omega)d\omega=1$. In this particular case, there is no straightforward spectral function for describing the magnetic data. At low temperatures the spectrum is certainly not Lorentzian, and above 50 K the spectra cannot be described by one line either (compare 17 and 69-meV spectra in Figs. 4 and 5). However, for the calculation of the static susceptibility, the scattering function has to be brought within parameters according to Eq. (1). We did that by fitting the spectra with several empirical inelastic lines, with the sole restriction that the same parameters had to describe the 17- and 69-meV data [Q independence was assumed, i.e., $P(\mathbf{Q},\omega)=P(\omega)$]. The static susceptibility, calculated from the neutron data, reproduce the temperature dependence of the bulk susceptibility (see solid circles in Fig. 1). Since the neutron susceptibility in absolute units exceed the susceptometer values by about 15%, we have scaled them to the 100-K value of the bulk susceptibility. However, the integrated magnetic intensity in absolute units of cross section underestimates the Ce^{3+} cross section by 30%. Having in mind that the integrated magnetic intensity is given by $\sigma_{\text{mag}}=4\pi\int_{-\infty}^{\infty}S(Q,\omega)d\omega$ (more or less the area under the spectra), and that the static susceptibility takes into account magnetic intensities according to $1/\omega$ (the bigger the energy transfer the smaller the contribution to χ), we draw the following conclusion: we have correctly determined the magnetic intensity in the energy window covered (≤ 60 meV) but possibly have missed intensity at energy transfers beyond 60 meV.

DISCUSSION

The broad structureless magnetic response of $Ce_3Bi_4Pt_3$ beyond 20 meV compares well with the spectra of metallic intermediate-valence compounds,[14–18] however, a magnetic gap as found in $Ce_3Bi_4Pt_3$, has not yet been reported for any Ce compound. Therefore, we will start with a brief comparison of our neutron-scattering results and the ones of related compounds that exhibit a gap in their electronic spectrum. To our knowledge only neutron data of TmSe (Ref. 20) and SmB_6 (Ref. 21) have been published. TmSe is not well suited for a comparison since, in Tm, as opposed to Ce, Sm, and Yb, two magnetic $4f$ configuration are involved, and for SmB_6 no statement can be made concerning the existence of a magnetic gap from the existing data.[21] However, the behavior found in $Ce_3Bi_4Pt_3$ seems to be confirmed by preliminary CeNiSn (Ref. 22) and YbB_{12} (Ref. 23) data. In both cases, a gap appears to be present in the magnetic excitation spectrum with $\Delta_m\geq\Delta$. These observations immediately raise two questions: (1) What is the origin of the magnet-

ic gap? (2) What is the relationship between the magnetic gap Δ_m and the transport gap Δ?

To address the possible appearance of a gap in the spin-spin correlation function, with $\Delta_m > \Delta$, we present the following simple model—although it is not at all clear that this model contains all the essential physics: the dynamic susceptibility $\chi(\mathbf{Q},\omega)$ has been calculated within the framework of the spin-1/2 Anderson Lattice model. For the intra-atomic Coulomb repulsion $U=0$, this model reduces to an effective two-band model, each band containing states of mixed f and d characters and holding an integral number of electrons per $4f$ ion. These bands are separated by a gap which becomes the hybridization gap if the f-level is degenerate with the nonhybridized d-band. The electronic system is semiconducting-like if the chemical potential μ lies in the gap. However, because $\chi(\mathbf{Q},\omega)$ is a two-particle correlation function, it does not probe the electronic structure directly. The dynamic susceptibility contains four contributions due to electron-hole excitations. Two interband contributions involve the electron and hole excitations in different bands; specifically, one occurs when an electron is excited to the upper band and the hole to the lower one, the other contribution of this type is only allowed at finite temperature when there is a thermal population of electrons in the upper and of holes in the lower band. The other two intraband contributions involve only the electron-hole excitations which are both restricted to occur within either the upper or lower hybridized band and, therefore, can only represent real excitations at finite temperatures. At temperatures on the order of the transport gap Δ, the intraband contribution produces a maximum in $\chi_{\text{stat}}=\text{Re}\chi(0,0)$ due to the presence of electron-hole pairs in the peaks of the hybridized density of states.

The inelastic, paramagnetic neutron-scattering cross section is related to $(1-\exp[-\hbar\omega/kT])^{-1}\chi''(\mathbf{Q},\omega)$ by Eq. (1). At low temperatures, the only allowed electron-hole spin-flip excitation processes that are expected to contribute are the interband transitions. These have a minimum excitation energy threshold that is dependent on $\mathbf{Q}$ and that varies from V^2/W at $\mathbf{Q}=(\pi/a)(1,1,1)$ to $2V$ at $\mathbf{Q}=\mathbf{0}$, where V is the hybridized matrix element and W is the unhybridized d-band width. As a result, the observed threshold in the magnetic spectrum is greater than the gap inferred from thermodynamic measurements. Above the threshold energy, a peak in the inelastic neutron cross-section can be interpreted as indicating the existence of at least one peak in the hybridized density of states, near the edges of the gap. At higher temperatures, when the hybridized bands do have significant thermally induced populations of electrons or holes, the intraband contribution to $\chi''(\mathbf{Q},\omega)$ can be expected to become important. These will give rise to a quasielastic contribution, with a thermally activated integrated intensity. Thus, at higher temperatures, one would expect that intensity in the gap region should become apparent, resulting in a gradual filling of the gap. However, the experimental data of Figs. 4 and 5 are more consistent with a rapid closing of the gap between 50 and 100 K; that is, the gap itself appears to be temperature dependent. Indeed, there is evidence for a temperature dependence of the transport gap as well, with $d\Delta/dT<0$. A temperature dependence of the gap is expected from the slave-boson theory, in the mean-field approximation; unfortunately, in the metallic case it gives rise to an unphysical phase transition to a localized phase.[24,25] An alternative explanation could be the presence of a low-energy collective spin-fluctuation mode in the gap, which at finite temperatures broadens due to Raman-like scattering processes, thereby filling the gap. However, the apparent absence of such a collective mode in the low-temperature magnetic excitation spectrum makes this explanation unlikely.

In order to be more quantitative, the model would have to contain more realistic assumptions as, for example, a temperature-dependent hybridization. Furthermore, including the full degeneracy of the $J=\frac{5}{2}$ manifold may be an important consideration since there is no evidence for crystal-field splitting. For a direct comparison between theory and experiment, it will be essential to determine experimentally the $\mathbf{Q}$ dependence of Δ_m.

CONCLUSION

We have found incontrovertible evidence for a gap Δ_m in the magnetic excitation spectrum of $Ce_3Bi_4Pt_3$ that is larger than the gap inferred from transport measurements. Above ≈ 50 K, the gap begins to fill more rapidly than expected from Bose statistics alone, implying a fundamental temperature dependence of Δ_m, as also may be the case for the gap in the electronic excitation spectrum. We have applied a simple model that qualitatively accounts for the behavior of $\chi''(\mathbf{Q},\omega)$ and χ_{stat} but appears to be too simple to explain these behaviors quantitatively. The existence of a magnetic gap in other systems similar to $Ce_3Bi_4Pt_3$ suggests that this is a general phenomenon. The extent to which the magnetic gap in these semiconductor-like materials is related to that found in metallic $YbAl_3$ is an open question, but qualitatively they appear similar.

ACKNOWLEDGMENT

The work at Los Alamos was performed under the auspices of the U.S. Department of Energy.

[1]M. F. Hundley, P. C. Canfield, J. D. Thompson, Z. Fisk, and J. M. Lawrence, Phys. Rev. B **42**, 6842 (1990). In this reference the activation energy Δ was defined from the resistivity through $\rho \propto e^{-\Delta/kT}$. Throughout this paper we use the terms activation energy and energy gap interchangeably.

[2]G. H. Kwei, J. M. Lawrence, P. C. Canfield, W. P. Beyermann, J. D. Thompson, A. C. Lawson, and J. A. Goldstone, (unpublished).

[3]P. Haen, F. LaPierre, J. M. Mignot, and R. Tournier, Phys. Rev. Lett. **43**, 304 (1979).

[4]A. Jayaraman, V. Narayanamurti, E. Bucher, and R. G. Maines, Phys. Rev. Lett. **25**, 1430 (1970).
[5]T. Kasuya, F. Iga, M. Takigawa, and T. Kasuya, J. Magn. Magn. Mater. **47&48**, 429 (1985).
[6]G. P. Meisner, M. S. Torikachvili, K. N. Yang, M. B. Maple, and R. P. Guertin, J. Appl. Phys. **57**, 3073 (1985).
[7]T. Takabatake, F. Teshina, H. Fujii, S. Nishigori, T. Suzukli, T. Fujita, Y. Yamaguchi, J. Sakurai, and D. Jaccard, Phys. Rev. B **41**, 9607 (1990).
[8]S. K. Malik and D. T. Adroja, Phys. Rev. B **43**, 6267 (1991).
[9]U. Walter and E. Holland-Moritz, Z. Phys. B **45**, 107 (1981).
[10]B. Frick and M. Loewenhaupt, Z. Phys. B **63**, 213 (1986); **63**, 231 (1986).
[11]A. P. Murani, Phys. Rev. Lett. **41**, 1406 (1978).
[12]S. Horn, F. Steglich, M. Loewenhaupt, and E. Holland-Moritz, Physica B **107**, 103 (1981).
[13]A Severing, A. P. Murani, J. D. Thompson, Z. Fisk, and C.-K. Loong, Phys. Rev. B **41**, 1739 (1990).
[14]R. M. Galera, D. Givord, J. Pierre, A. P. Murani, C. Vettier, and K. R. A. Ziebeck, J. Magn. Magn. Mater. **47&48**, 138 (1985).
[15]A. Severing and A. P. Murani, Physica B **163**, 699 (1990).
[16]C.-K. Loong, B. H. Grier, S. M. Shapiro, J. M. Lawrence, R. D. Parks, and S. K. Sinha, Phys. Rev. B **35**, 3092 (1987).
[17]A. Severing, E. Gratz, B. D. Rainford, and K. Yoshimura, Physica B **163**, 409 (1990).
[18]A. P. Murani, Phys. Rev. Lett. **54**, 1444 (1985).
[19]A. P. Murani (unpublished).
[20]M. Loewenhaupt and E. Holland-Moritz, J. Appl. Phys. **50**, 7456 (1979).
[21]E. Holland-Moritz and M. Kasaya, Physica B **136**, 424 (1986).
[22]T. E. Mason, C. Broholm, G. Aeppli, K. N. Clausen, N. Stückli, and E. Bucher (unpublished).
[23]M. Bonnet, A. Bouvet, M. Kasaya, T. Kasuya, J. Rossat-Mignod, and A. Severing (unpublished).
[24]P. Coleman, Phys. Rev. B **35**, 5072 (1987).
[25]O. Valls and Z. Tesanovich, Phys. Rev. B **34**, 1918 (1987).